JACS
JOURNAL OF THE AMERICAN CHEMICAL SOCIETY
pubs.acs.org/JACS
Article

Light-Promoted C(sp^3)–C(sp^3) Reductive Elimination from Dialkyl Ni^{II} Complexes

Alexander Q. Cusumano,[‡] Braden C. Chaffin,[‡] David A. Cagan,[⊥] Stephen DiLuzio,[⊥] Erica Sutcliffe,[⊥] Ryan G. Hadt,[*] and Abigail G. Doyle[*]

Cite This: https://doi.org/10.1021/jacs.5c09925
Read Online

ABSTRACT: Ni-catalyzed cross-coupling is a powerful strategy to forge C(sp^3)–C(sp^3) bonds. Typically, to do so requires overcoming a challenging C–C bond-forming reductive elimination, often enabled by the intermediacy of highly oxidized Ni species or outer-sphere processes. While direct C(sp^3)–C(sp^3) reductive elimination from the Ni^{II} base oxidation state is normally thermally inaccessible, light-activation provides an avenue to affect such transformations. Here, we investigate the mechanism of light-induced C(sp^3)–C(sp^3) bond formation from dialkyl bipyridine Ni^{II} complexes through a variety of organometallic, spectroscopic, and computational studies. Wavelength-dependent quantum yields, ligand electronics–reactivity relationships, excited-state lifetimes, computed barriers, and product distributions from crossover studies support a photolysis/radical rebound mechanism. This reactivity paradigm complements existing strategies in the literature to promote reductive elimination from Ni^{II}, such as the use of destabilizing, sterically hindered ligands and reduction of electron density at Ni through the binding of electron-deficient olefins. Hence, we envision that light-induced reductive elimination may enable the development of challenging C(sp^3)–C(sp^3) couplings.

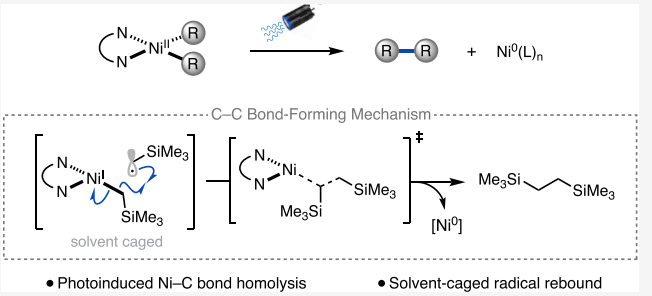

INTRODUCTION

The integration of photochemistry with first-row transition metal catalysis has offered powerful strategies for the development of novel cross-coupling reactions.[1] Ni has emerged as a privileged catalyst for such applications due to its ability to access a range of oxidation states, enabling both one- and two-electron processes, and relative reluctance to undergo decomposition pathways, such as β-hydride elimination from catalytic intermediates bearing alkyl fragments.[2] While the past decade has seen substantial development in methods that employ a separate photocatalyst to mediate redox or energy transfer events within a formally light-independent Ni catalytic system,[3] recent developments highlight that Ni itself possesses unique photochemical reactivity that enables catalysis.[4]

Independent reports from our two laboratories demonstrated that exposure of (bipyridine)Ni^{II}(aryl)(halide) complexes to blue/violet light leads to Ni^{II}–C(sp^2) homolysis, yielding Ni^{I} and $^{\bullet}$C(sp^2), via repulsive triplet ligand-to-metal charge transfer (LMCT) states (Figure 1A).[5] Analogous reactivity has been reported from (bipyridine)$Ni^{II}(X)_2$ complexes (X = Cl, Br) (Figure 1A).[6] This photolysis from thermodynamically stable Ni^{II} intermediates has been hypothesized as a key process in accessing catalytically active Ni^{I} species for productive Ni^{I}/Ni^{III} catalytic cycles.[7] Moreover, in the case of $Ni^{II}(X)_2$ complexes (X = Cl, Br), the liberated halogen atom ($X^{\bullet}$) can serve to activate a substrate, such as the generation of alkyl radicals from halogen atom-mediated C(sp^3)–H hydrogen atom transfer (HAT).[8]

In addition to catalyst or substrate activation, irradiation of Ni^{II} complexes has been demonstrated to promote bond formation. Park and co-workers found that irradiation of (bpy)Ni^{II}(Me)(SPh) (**1**) leads to the evolution of ethane in 62% yield, likely through the liberation of methyl radical ($Me^{\bullet}$) (Figure 1B).[9] Irradiation of metalacyclic complex **2** affords exclusively intramolecular C–S bond formation in quantitative yield.

Light-induced bond formation has been proposed to occur via canonical reductive elimination transition states from triplet metal-to-ligand charge transfer (^{3}MLCT) electronic states (Figure 1C). Following experimental studies by MacMillan and co-workers,[10] computational investigations by Chen and Guan offered support for such a mechanism in the C–O bond formation from bipyridine Ni^{II} aryl carboxylate complexes.[11] Recently, calculations by Rueping and Cavallo also highlight

Received: June 12, 2025
Revised: August 15, 2025
Accepted: August 18, 2025

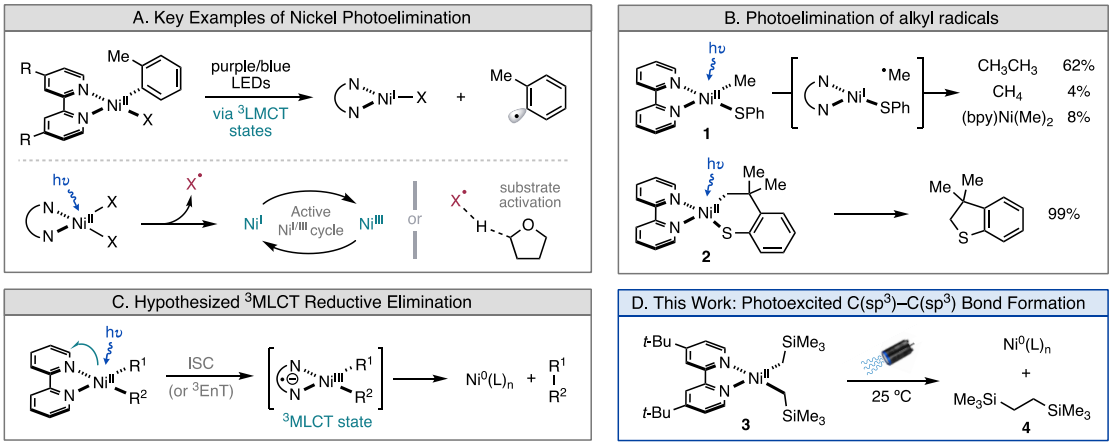

Figure 1. Photochemical reactivity of Ni^{II} complexes relevant to catalysis.

the possibility of such a step for $C(sp^3)-C(sp^3)$ bond formation from a proposed Ni^{II} bis-alkyl intermediate in a Ni-catalyzed photochemical $C(sp^3)-H$ alkylation.[12] In a related system, in the context of $C(sp^2)-C(sp^3)$ bond formation, our group sought to experimentally evaluate this hypothesis through organometallic synthesis and stoichiometric photochemical studies on isolated ($^{t\text{-Bu}}$bpy)Ni^{II}(*o*-Tol)-(CH_2SiMe_3).[8a] Indeed, 427 nm irradiation dramatically increased the rate of $C(sp^2)-C(sp^3)$ bond formation, affording the cross-coupled organic product in 32% yield after 60 min. The high selectivity for $C(sp^2)-C(sp^3)$ coupling led us to postulate a concerted reductive elimination from a ^{3}MLCT state; however, the contrast in product distribution from that of **1** was intriguing.

Given the importance of Ni-catalyzed C−C cross-coupling reactions, and the inherent challenge of forging $C(sp^3)-C(sp^3)$ bonds from the Ni^{II} oxidation state,[13,14] we sought to further interrogate the nuclear and electronic mechanisms, scope, and reactivity trends of light-promoted $C(sp^3)-C(sp^3)$ bond formation from Ni^{II} dialkyl complexes (Figure 1D). Here, we present our spectroscopic, photochemical, computational, and organometallic studies to differentiate between several plausible mechanistic hypotheses for light-promoted bond formation from Ni^{II}. Our investigations support a unimolecular C−C bond formation involving a solvent-caged radical rebound mechanism, initiated by homolysis of the Ni−C bond via repulsive ^{3}LMCT excited states. Lastly, we find that light-activation is complementary to prior strategies in the literature in promoting $C(sp^3)-C(sp^3)$ reductive elimination from a Ni^{II} center, proceeding without the need for designer ligands or introduction of strong π-accepting ancillary ligands. This expansion of fundamental understanding of Ni photochemistry reactivity principles offers opportunities for the development of new catalytic transformations involving $C(sp^3)-C(sp^3)$ cross-coupling

RESULTS AND DISCUSSION

In our prior investigation of the mechanism of Ni-catalyzed photochemical halogen atom-mediated $C(sp^3)-H$ arylation of alkyl ethers, we observed the ability for blue light irradiation to promote $C(sp^2)-C(sp^3)$ reductive elimination from the model complex ($^{t\text{-Bu}}$bpy)Ni^{II}(*o*-Tol)(CH_2SiMe_3).[8a] Despite ultimately finding that reductive elimination in this particular reaction likely occurs from a different catalytic species, the ability for visible light irradiation to promote C−C coupling from Ni^{II} was intriguing. Preliminary investigations showed this reactivity paradigm could be extended to $C(sp^3)-C(sp^3)$ bond formation as well, with 427 nm blue LED irradiation of the dialkyl complex ($^{t\text{-Bu}}$bpy)$Ni^{II}(CH_2SiMe_3)_2$ (**3**), forging 1,2-bis(trimethylsilyl)ethane (**4**) (Figure 2). While recent efforts by our group and others highlight the role of bipyridine Ni photochemistry as a means of catalyst or substrate activation,

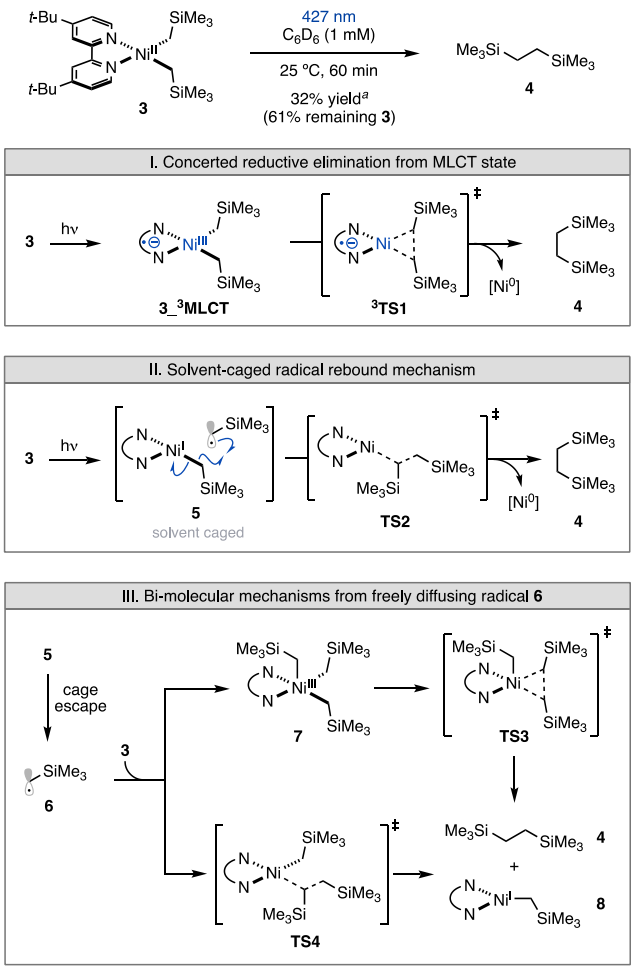

Figure 2. Initial findings and potential mechanisms for the $C(sp^3)-C(sp^3)$ bond formation. (a)^{1}H NMR yield based on a toluene internal standard.

https://doi.org/10.1021/jacs.5c09925
J. Am. Chem. Soc. XXXX, XXX, XXX−XXX

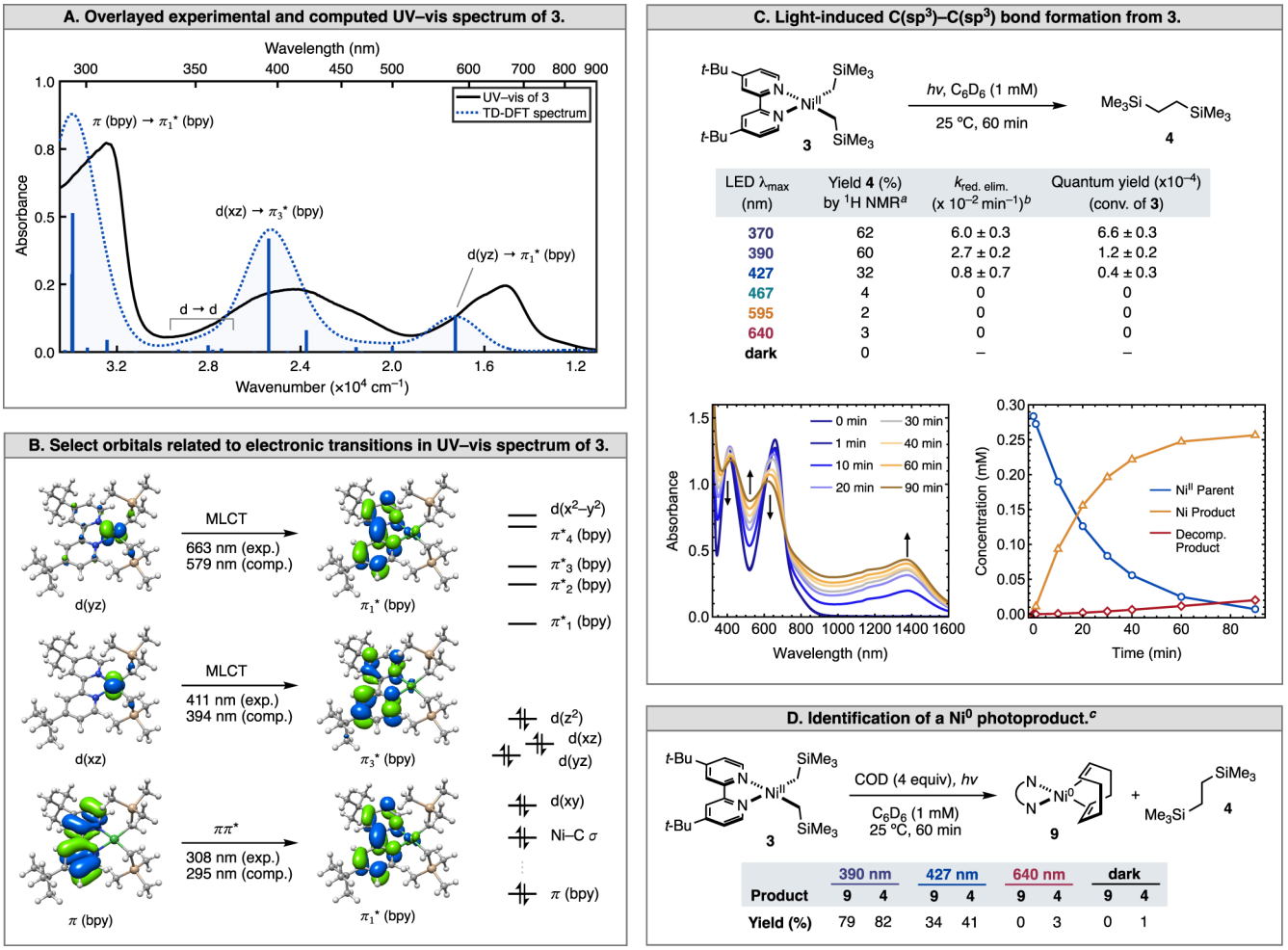

LED λ_{max} (nm)	Yield **4** (%) by ^{1}H NMR[a]	$k_{red.\ elim.}$ ($\times 10^{-2}$ min^{-1})[b]	Quantum yield ($\times 10^{-4}$) (conv. of **3**)
370	62	6.0 ± 0.3	6.6 ± 0.3
390	60	2.7 ± 0.2	1.2 ± 0.2
427	32	0.8 ± 0.7	0.4 ± 0.3
467	4	0	0
595	2	0	0
640	3	0	0
dark	0	–	–

	390 nm		427 nm		640 nm		dark	
Product	9	4	9	4	9	4	9	4
Yield (%)	79	82	34	41	0	3	0	1

Figure 3. (A) UV−vis absorption spectrum of **3** in benzene (50 mM), showing low- and high-energy MLCT bands, and bpy $\pi \rightarrow \pi^*$ transitions at 663, 411, and 308 nm, respectively. Overlayed TD-DFT calculated spectrum (TPSSh-D4/def2-TZVPP/CPCM(benzene)//PBE-D4/def2-TZVP(Ni),def2-SV(P)/CPCM(benzene)) (Supporting Information, Section 7). (B) Qualtitative molecular orbital diagram and relevant orbital isosurfaces and electronic transitions are depicted. (C) Wavelength-dependent photochemistry of **3**. (a) ^{1}H NMR yield based on toluene internal standard. (b) Rate constant and quantum yield for conversion of **3** were derived from UV−vis kinetics (Supporting Information, Section 9). Note that mass balance is generally well preserved, and **4** and **5** are formed in 1:1 stoichiometry. (D) Photolysis in the presence of COD affords ($^{t\text{-Bu}}$bpy)Ni^0(COD) (**9**) as the Ni photoproduct. (c) ^{1}H NMR yield based on toluene internal standard.

the ability to employ light to promote C(sp^3)−C(sp^3) bond formation from Ni^{II} represents an exciting development in our understanding of Ni photochemistry. Hence, we sought to explore the mechanism and scope of this reactivity paradigm.

Building upon prior studies and literature insights, there are several reasonable mechanisms for photoexcited bond formation. For example, studies by Diao and co-workers demonstrate that single-electron oxidation of *N,N*-ligated dialkyl Ni^{II} complexes to their cationic Ni^{III} counterparts enables facile reductive elimination to forge C(sp^3)−C(sp^3) bonds.[15] Considering the redox noninnocent nature of the bipyridine ligands,[16] an analogous Ni^{III} configuration can be transiently achieved via light-induced metal-to-ligand charge transfer (MLCT) (Figure 2I). A three-centered reductive elimination (^{3}**TS1**) would then ensue from this MLCT excited state.[11]

Prior studies by our groups[5] and Park and co-workers[9] have demonstrated that bipyridine aryl halide complexes undergo Ni−C(sp^2) homolysis upon irradiation with high-energy light (≲427 nm). Hence, we envisioned an alternative mechanism in which irradiation promotes Ni−CH_2SiMe_3 homolysis (to **5**), followed by rapid radical rebound and C−C bond formation via an S_H2-like process (**TS2**) (Figure 2II).[17] The nature of this process may range from a highly asynchronous three-centered reductive elimination to a stepwise radical ejection/outer-sphere C−C bond formation, but wherein both Ni^I and organic radical remain in the solvent cage.[18]

Alternatively, if the S_H2-like bond formation is slow, then cage escape can prevail (Figure 2III). The freely diffusing neosilyl radical (**6**) may add to another equivalent of **3** to forge ($^{t\text{-Bu}}$bpy)Ni^{III}(CH_2SiMe_3)$_3$ (**7**), which undergoes reductive elimination (**TS3**) to yield organic product **4** and Ni^I (**8**). A mechanism featuring an outer-sphere S_H2-like bond formation (via **TS4**) is also possible.

Mechanistic Studies. The key to uncovering the reductive elimination mechanism is understanding the underlying photophysical processes that are accessible to these complexes. Thus, we sought to examine the electronic transitions available to **3**. The UV−vis spectrum of **3** in benzene features two broad absorbances with λ_{max} at 411 nm (ε = 4.7 × 10^3 M^{-1} cm^{-1}) and 663 nm (ε = 4.9 × 10^3 M^{-1} cm^{-1}) (Figure 3A). Time-dependent density functional theory (TD-DFT) calculations

https://doi.org/10.1021/jacs.5c09925
J. Am. Chem. Soc. XXXX, XXX, XXX−XXX

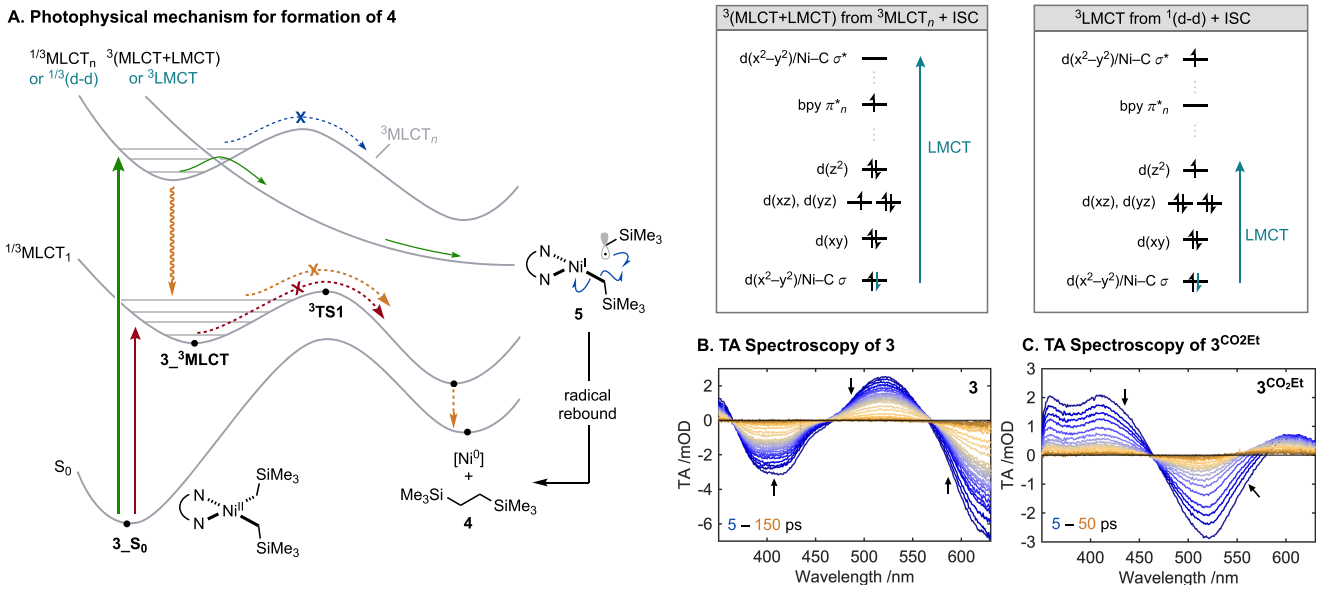

Figure 4. (A) Generalized photophysical mechanisms for C−C bond formation from dialkyl Ni^{II} complexes. The nature of the repulsive triplet surface leading to **5** is either ^{3}(MLCT+LMCT) or ^{3}LMCT depending on whether the states were accessed from ^{1}MLCT or ^{1}(d-d) manifolds, respectively.[5b] Note that MLCT refers to Ni to bipyridine CT, whereas LMCT refers to Ni−Cσ to Ni CT. Transient absorption spectra of (B) **3** and (C) $\mathbf{3}^{\mathbf{CO2Et}}$ at longer time scales following 700 and 800 nm photoexcitation, respectively, likely showing relaxation to the ground state from a relaxed MLCT state.

suggest that the low-energy absorption corresponds primarily to a metal-to-ligand charge transfer (MLCT) from the metal-based d(yz) donor to the bipyridine π_1* acceptor (Figure 3B). Other MLCT transitions to the bipyridine π_1* acceptor are similar in energy but are characterized by significantly lower oscillator strengths (Supporting Information, Section 7). The largest of the MLCT oscillator strengths belongs to the d(xz) to bipyridine π_3*, which is the major contributor to the absorbance feature at 411 nm. The ^{1}(d-d) ligand-field transitions are computed at 341−364 nm and are slightly mixed with MLCT character. Bipyridine-based π to π* transitions are observed at 308 nm (ε = 1.6 × 10^4 M^{-1} cm^{-1}). Hence, the 427 nm LED that was shown to promote bond formation may access both high-energy MLCT states and ligand-field transitions, albeit with a smaller absorbance cross section for the latter.

Considering our initial hypothesis of bond formation from an MLCT state (Figure 2I), we envision a mechanism involving blue light (427 nm) promotion to a high-energy MLCT state, followed by intersystem crossing (ISC) and internal conversion (IC) to a low-lying ^{3}MLCT state. The lowest energy triplet state is of MLCT character (d(z^2) → bpy π_1*) with vertical and adiabatic excitation energies computed to be 30.0 and 15.0 kcal/mol, respectively (Supporting Information, Section 7).[19] Hence, irradiation at longer wavelengths (~600−700 nm) targeting the low-energy MLCT manifold should also intercept this mechanism and affect C−C bond formation. However, negligible reactivity was observed upon exposure to 467−640 nm light (Figure 3C). Conversely, irradiation at shorter wavelengths (370 and 390 nm) roughly doubled conversion, affording 60−62% yield of **4** after 1 h. As described above, unreacted **3** represents the remaining mass balance. Reaction progress was also followed by UV−Vis spectroscopy to determine wavelength-dependent rate constants and quantum yields for the consumption of **3**. In accord with shorter wavelength irradiation (390 and 370 nm) leading to an increased yield of **4**, the quantum yield for consumption of **3** also increased with decreasing wavelength (Figure 3C).

Introduction of 1,5-cyclooctadiene (COD) allows for quantification of ($^{t\text{-Bu}}$bpy)Ni^0(COD) (**9**) as a soluble, well-defined organometallic photoproduct (Figure 3D). Irradiation of **3** in the presence of COD at 390 nm affords a nearly 1:1 ratio of organic product **4** and ($^{t\text{-Bu}}$bpy)Ni^0(COD) (**9**) in 79% and 82% yield, respectively, as determined by ^{1}H NMR (Figure 3D).[20] Across all wavelengths evaluated, **9** is formed in essentially a 1:1 stoichiometric ratio with the organic product **4**.

These results are not consistent with a Kasha process involving reductive elimination from a low-energy ^{3}MLCT state (red pathway, Figure 4A). Moreover, a thermal barrier of 19.4 kcal/mol is computed along the lowest energy adiabatic triplet potential energy surface ($\mathbf{3}\_^3\mathbf{MLCT}_1$ to ^{3}**TS1**, Figure 4A). From the ground vibrational state, $\mathbf{3}\_^3\mathbf{MLCT}_1$ would likely have an insufficient lifetime to undergo reductive elimination via ^{3}**TS1**. We postulated that the population of a vibronic state of $\mathbf{3}\_^3\mathbf{MLCT}_1$, more closely matched in energy to ^{3}**TS1** (i.e., via IC from $^3\mathbf{MLCT}_n$, orange path in Figure 4), may enable bond formation. However, irradiation at excitation wavelengths above this energetic cutoff (within the entirety of the low-energy MLCT band) fails to afford the product.

To better understand the excited-state dynamics of the system, transient absorption studies were carried out on complexes **3** and (^{CO2Et}bpy)$Ni(CH_2SiMe_3)_2$ ($\mathbf{3}^{\mathbf{CO2Et}}$) (Figure 4B-C). With both 400 and 700 nm pump wavelengths, two components in the excited-state dynamics are observed, with ~2 and ~19 ps (Figure 4B). We attribute these processes to IC/ISC to a relaxed MLCT state and subsequent recovery back to the ground state, respectively. The latter process is shown in Figure 4B, where the excited-state absorption is indicative of a reduced bpy species that decays at the same rate as the recovery of the ground state bleach. Complex $\mathbf{3}^{\mathbf{CO2Et}}$ presents excited-state dynamics similar to that of 3, with corresponding time constants of ~3 and ~11 ps across 800

https://doi.org/10.1021/jacs.5c09925
J. Am. Chem. Soc. XXXX, XXX, XXX−XXX

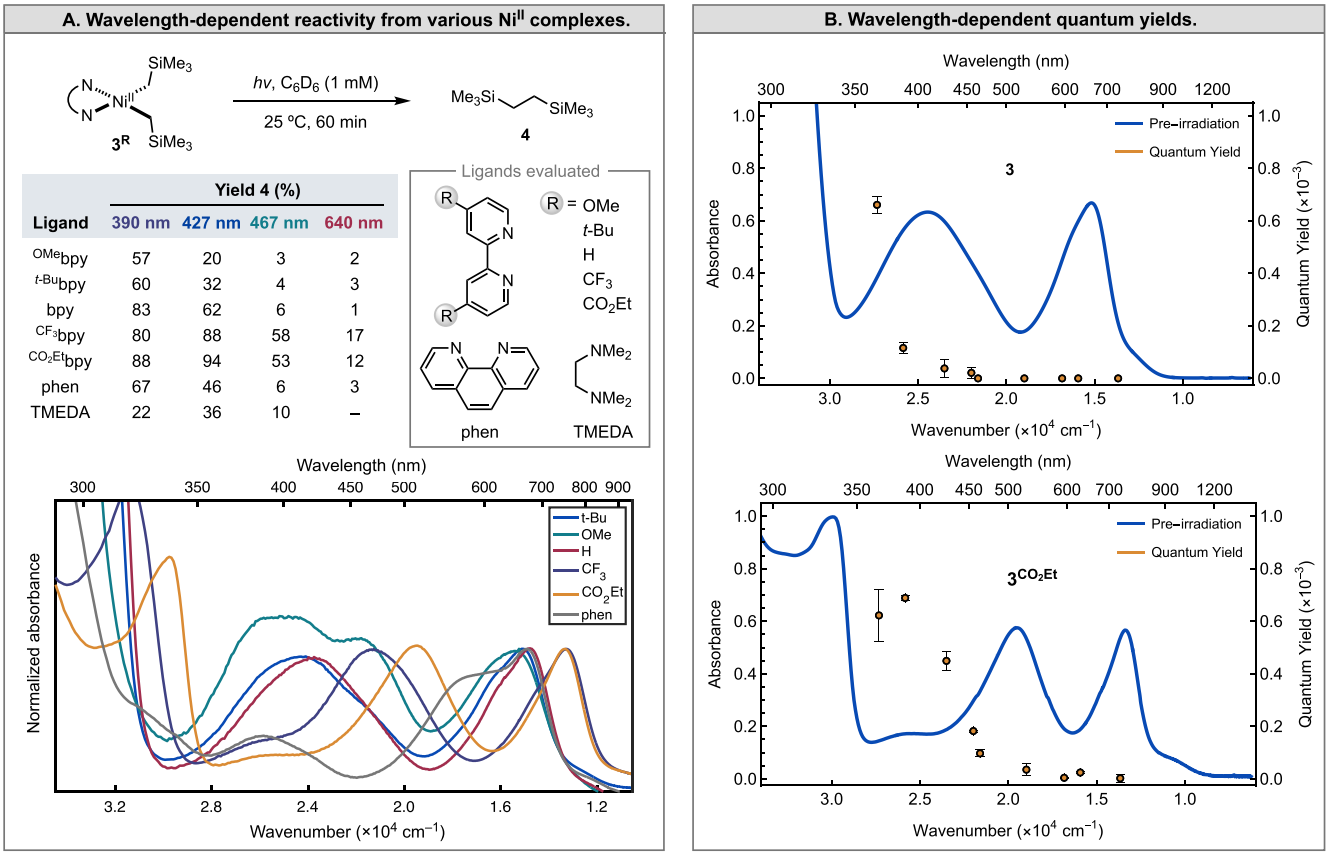

Figure 5. (A) Light-induced C−C bond formation as a function of ligand electronics and the irradiation wavelength. Photolysis reactions were run at 25 °C in C_6D_6 (1 mM) for 60 min. ^{1}H NMR yield based on the toluene internal standard. (B) Plots of wavelength-dependent quantum yields for **3** and $\mathbf{3}^{\mathbf{CO2Et}}$.

and 530 nm pump wavelengths (Supporting Information, Section 10). This behavior is distinct from that of bipyridine Ni^{II}(aryl)(halide) complexes, which decay through a long-lived ($\tau \sim$ ns) ^{3}(d-d) state.[5a] Given the short lifetimes of the $MLCT_n$ states of **3**, an anti-Kasha reductive elimination (blue pathway, Figure 4A) is also unlikely.

While the absorption profile of **3** between 320−500 nm is characterized by bright, high-energy MLCT transitions, ^{1}(d-d) states are also present in this portion of the excited-state manifold. To determine which states ultimately give rise to productive bond formation, we sought to perturb the ancillary bpy ligand framework to energetically separate the various classes of electronic transitions. To this end, we prepared a library of dialkyl Ni^{II} complexes varying the electronics of the bpy ligand (R = OMe, *t*-Bu, H, CF_3, and CO_2Et) (Figure 5A). Electron-withdrawing groups on the bipyridine backbone serve to stabilize the ligand-based radical anion character of the MLCT states.[16] This is reflected in the red-shift of both high- and low-energy MLCT bands in the UV−vis spectra of (^{CO2Et}bpy)$Ni^{II}(CH_2SiMe_3)_2$ ($\mathbf{3}^{\mathbf{CO2Et}}$) and (^{CF3}bpy)-$Ni^{II}(CH_2SiMe_3)_2$ ($\mathbf{3}^{\mathbf{CF3}}$). Meanwhile, our calculations suggest the energies of the ligand-field transitions are only minimally perturbed by these ligand substitutions (Supporting Information, Section 7). As an additional point of comparison, phenanthroline complex $\mathbf{3}^{\mathbf{phen}}$ was also prepared, as it offers a large absorbance cross section between 500 and 700 nm, while featuring an otherwise similar ligand framework and thermal stability.

Complexes $\mathbf{3}^{\mathbf{OMe}}$, $\mathbf{3}^{\mathbf{H}}$, and $\mathbf{3}^{\mathbf{phen}}$ show comparable reactivity to **3** ($\mathbf{3}^{\mathbf{t\text{-}Bu}}$), with C−C bond formation occurring upon ≤427 nm irradiation. Analogously, $\mathbf{3}^{\mathbf{CO2Et}}$ and $\mathbf{3}^{\mathbf{CF3}}$ both demonstrate wavelength-dependent reactivity; however, substantial reactivity persists even at 467 nm irradiation, affording **4** in 53 and 58% yield, respectively. Interestingly, compared to **3**, the wavelength-dependent quantum yields from $\mathbf{3}^{\mathbf{CO2Et}}$ reveal that maximum quantum yield does not follow the red-shift in the high-energy MLCT band (411 → 511 nm), with the highest quantum yields still obtained at 370−390 nm irradiation (Figure 5B). This observation is also inconsistent with the aforementioned hypothesis, in which reductive elimination occurs from a vibronically excited $MLCT_1$ state that is the direct product of internal conversion from a higher-energy $MLCT_n$ state (orange pathway, Figure 4A). As a mechanism involving reductive elimination directly from an MLCT state is thus far inconsistent with experimental evidence, we sought to evaluate whether productive reactivity could be initiated from non-MLCT states.

To independently probe reactivity from the initial population of a ligand-field manifold, we prepared the tetramethylethylenediamine complex (TMEDA)-$Ni^{II}(CH_2SiMe_3)_2$ ($\mathbf{3}^{\mathbf{TMEDA}}$), whose bidentate *N,N*-ligand offers no accessible MLCT transitions. The ^{1}(d-d) transitions of $\mathbf{3}^{\mathbf{TMEDA}}$ are computed at 424−473 nm (Table S6), corresponding well to the experimental UV−vis spectrum with λ_{max} at 453 nm ($\varepsilon = 4.3 \times 10^2$ M^{-1} cm^{-1}) (Figure S21). Interestingly, irradiation of $\mathbf{3}^{\mathbf{TMEDA}}$ with 427 nm light *does* afford cross-coupled product **4** in 36% yield after 1 h.

https://doi.org/10.1021/jacs.5c09925
J. Am. Chem. Soc. XXXX, XXX, XXX−XXX

Irradiation at 390 and 467 nm also affords the product in 22 and 10% yield, respectively. These results suggest that ^{1}(d-d) excitations also lead to C−C bond formation.

Wavelength-dependent photochemical reactivity of Ni^{II} organometallics from both MLCT and ligand-field states is reminiscent of findings from prior studies by our group exploring the mechanism of Ni−C(sp^2) photolysis from (^{R}bpy)Ni^{II}(aryl)(halide) complexes.[5b] In these studies, we showed that the population of high-energy MLCT and ^{1}(d-d) states can feed to triplet LMCT (or MLCT + LMCT) states that are repulsive with respect to the Ni−C(sp^2) bond.[5b] These findings were in accord with studies by Park and co-workers that also find ^{1}(d-d) states responsible for Ni−C(sp^3) homolysis from a variety of metallacyclic and acyclic Ni^{II} complexes, with redox active (bpy) and inactive (TMEDA, 1,2-bis(dimethylphosphineo)ethane (dmpe)) ligands.[9,21]

Due to this established photochemistry from Ni^{II}, we considered an alternative mechanism featuring Ni−C(sp^3) photolysis to form Ni^{I} and $^{\bullet}$C(sp^3) intermediates. However, after this initial step, two distinct mechanistic pathways can evolve based on the fate of the organic radical intermediate. First, the $^{\bullet}$C(sp^3) radical (**6**) may remain within the primary solvent cage and rapidly undergo an outer-sphere S_H2-like C−C bond formation with Ni^{I}(alkyl) intermediate **5** (Figure 2II). We refer to this process as a "radical rebound" process, given its analogy to the oxygen radical rebound mechanism in Fe-oxo C−H oxidation.[22] Alternatively, the $^{\bullet}$C(sp^3) radical (**6**) may freely diffuse, either adding to unreacted **3**, affording a Ni^{III} intermediate **7** from which reductive elimination occurs (**TS3**), or directly yield product **4** via an outer-sphere S_H2 mechanism (**TS4**) (Figure 2III).

Park and co-workers find that 390 nm irradiation of (bpy)Ni^{II}(Me)(SPh) and (dmpe)Ni^{II}(Me)(SPh) liberates Me$^{\bullet}$, affording ethane in 67 and 37% yield, respectively, yet thioanisol (MeSPh) was not detected.[9] These results are suggestive of the latter mechanism, involving a freely diffusing organic radical. However, in our prior study, we found irradiation of a differentially substituted alkyl/aryl complex ($^{t\text{-Bu}}$bpy)Ni^{II}(*o*-Tol)(CH$_2$SiMe$_3$) led exclusively to C(sp^3)−C(sp^2) bond formation. In this system, generation of a freely diffusing organic radical is improbable, as recombination with ($^{t\text{-Bu}}$bpy)Ni^{II}(*o*-Tol)(CH$_2$SiMe$_3$) and reductive elimination would likely lead to a mixture of C(sp^2)−C(sp^2), C(sp^3)−C(sp^2), and C(sp^3)−C(sp^3)-coupled products.[15]

To further probe the competition between radical rebound and diffusion, photolysis experiments were carried out in the presence of a second dialkyl Ni^{II} complex bearing different alkyl groups (Figure 6). ($^{t\text{-Bu}}$bpy)Ni^{II}(Me)$_2$ (**10**) and ($^{t\text{-Bu}}$bpy)-Ni^{II}(*n*-Bu)$_2$ (**11**) were paired with **3** in these crossover studies as their rates of photolysis are comparable to that of **3** at 390 nm. Irradiation of a 1:1 mixture of **3** and **10** affords predominantly direct coupling, with a 17% yield of ethyltrimethylsilane (**12**). The analogous reaction with **3** and **11** affords only 7% yield of the crossed product (**14**).[23] These results suggest the majority of photolysis events lead to C−C bond formation via rebound rather than cage escape, which would afford a more statistical mixture of products.

Moreover, it is also possible that radical diffusion may not directly lead to the formation of cross-products (Figure 2, Box III) but rather enables alkyl ligand exchange to reach mixed bis(alkyl) Ni^{II} intermediates. Prior studies demonstrate that C(sp^3)−C(sp^3) reductive elimination from five-coordinate Ni^{III} presents a sufficient barrier to observe the intermediacy

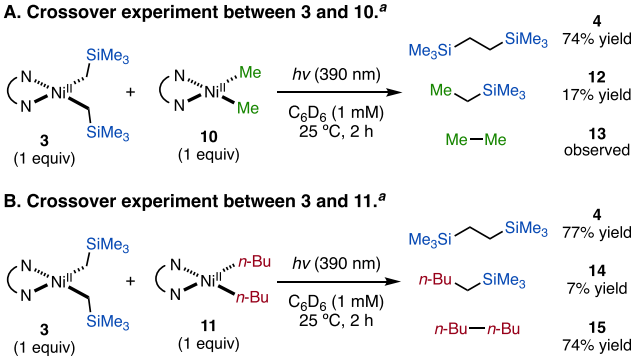

Figure 6. Crossover experiments under standard photolysis conditions (25 °C, overall 1 mM in C_6D_6) with two distinct dialkyl Ni complexes (both 0.5 mM in C_6D_6). (a) ^{1}H NMR yield based on toluene internal standard.

of such species.[24] Hence, a tris(alkyl) Ni^{III} intermediate that is the product of free radical capture by a dialkyl Ni^{II} complex may have sufficient lifetime to engage in comproportionation with photogenerated monoalkyl Ni^{I}, featuring the transfer of an alkyl ligand. From a mixed bis(alkyl) Ni^{II} species, a productive C−C bond formation via photolysis/radical rebound affords cross-products **12** and **14**.

Regardless, the productive radical rebound mechanism would quantitatively afford a Ni^0 product, whereas the direct product from the radical diffusion and capture mechanisms leading to C−C bond formation is Ni^{I}. As mentioned above, the introduction of COD to stabilize a low valent Ni photoproduct affords ($^{t\text{-Bu}}$bpy)Ni^0(COD) (**9**) in a 1:1 stoichiometric ratio with organic product **4** (Figure 3C). While it is possible that a ($^{t\text{-Bu}}$bpy)Ni^{I}(CH$_2$SiMe$_3$) (**8**) photoproduct could be disproportionate to Ni^{II} and Ni^0, the putative Ni^{I}(alkyl) intermediates would likely be highly unstable. Given the clean reaction profile and nearly quantitative mass balance, we suspect such a process is improbable for the major fraction of product formation. Indeed, the light-induced C−C bond-forming process likely directly affords a Ni^0 photoproduct alongside **4**.

Lastly, to address the possibility of a bimolecular mechanism,[25] we examined the dependence of the rate of bond formation on the concentration of **3**$^{\mathbf{CO2Et}}$. We find a first-order rate dependence on the concentration of **3**$^{\mathbf{CO2Et}}$, suggesting a mechanism with a unimolecular rate-limiting step (Supporting Information, Section 9).

In summary, we evaluated a number of mechanistic hypotheses for light-induced C(sp^3)−C(sp^3) bond formation from (^{R}bpy)Ni(CH$_2$SiMe$_3$)$_2$ complexes (Figure 2). Ultimately, cross-coupled product **4** is formed through a radical rebound mechanism, involving Ni−C(sp^3) photolysis (green path, Figure 4A) and subsequent S_H2-like C−C bond formation (Figure 2II).

Comparing Light-Induced Bond Formation to Alternative Reductive Elimination Strategies. The ability to forge C(sp^3)−C(sp^3) bonds via reductive elimination from Ni^{II} is an enabling elementary step for a variety of catalytic transformations. Thus, we examined the capabilities of this light-promoted bond formation in comparison to existing strategies in the literature to promote Ni^{II} reductive elimination, namely strategic ligand design[26] and use of electron-deficient olefins (EDOs) as added ancillary ligands.[14,27]

https://doi.org/10.1021/jacs.5c09925
J. Am. Chem. Soc. XXXX, XXX, XXX−XXX

Martin and co-workers demonstrated that modification of the steric properties of an ancillary ligand is a viable strategy to enable $C(sp^3)-C(sp^3)$ reductive elimination from dialkyl Ni^{II} complexes.[26] While phenanthroline-ligated complex (phen)-$Ni^{II}(CH_2SiMe_3)_2$ ($\mathbf{3}^{phen}$) is unreactive even upon heating to 100 °C for 24 h, introduction of 2,9-disubstitution on the ligand affords a complex (**16**, Figure 7) that readily evolves

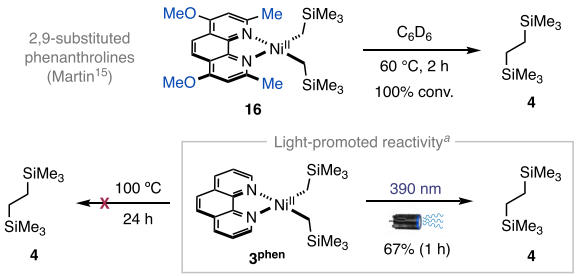

Figure 7. Comparison of ligand steric- and light-promoted reactivity from dialkyl Ni^{II} phenanthroline complexes. (a) ^1H NMR yield (25 °C, 1 mM in C_6D_6) based on the toluene internal standard.

cross-coupled product (**4**) at 60 °C. Martin found that the 2,9-disubstitution leads to significant distortion from square planarity, destabilizing **1**, enabling a more facile reductive elimination. However, given our findings with bipyridine ligands, we hypothesized that bond formation from $\mathbf{3}^{phen}$ could also be directly achieved by irradiation. Indeed, 390 nm irradiation of $\mathbf{3}^{phen}$ for 1 h at 25 °C evolves **4** in 67% yield (Figure 7). Hence, light-induced reductive elimination is an exciting alternative strategy to synthetically designed ligands for fashioning $C(sp^3)-C(sp^3)$ bonds.

Reducing the electron density at Ni through the binding of an electron-deficient olefin (EDO) is another strategy to enable $C(sp^3)-C(sp^3)$ reductive elimination. Seminal studies by Yamamoto and co-workers find that treatment of dialkyl bipyridine Ni^{II} complexes $(bpy)Ni^{II}(R)_2$ (R = Me, Et, etc.) with a variety of α,β-unsaturated carbonyl EDOs (acrolein, methyl vinyl ketone, etc.) readily promotes reductive elimination.[14] To our surprise, exposure of our model complex, $(^{t\text{-}Bu}bpy)Ni^{II}(CH_2SiMe_3)_2$ (**3**), to a variety of EDOs resulted in negligible reactivity, even at elevated temperatures (Figure 8A). While initially perplexing, we note that Yamamoto found that even small EDOs such as acrolein have highly unfavorable steric interactions with sterically hindered alkyl ligands such as *i*-Bu. Knochel has also reported the complement to be true, wherein large EDOs are hypothesized to fail to bind to even sterically unencumbered Ni complexes.[28] Thus, we suspected that the lack of EDO-promoted reductive elimination may arise from a disfavorable binding to **3** due to the imposing sterics of the neosilyl ligands. Indeed, ^1H NMR titration experiments with dimethylfumarate (**19**) as a representative EDO do not indicate any interaction with Ni (Figure 8B). For comparison, we prepared metallacycle **20** as a sterically accessible analog that is amenable to titration studies, as the cyclic structure prevents reductive elimination due to ring strain. Indeed, **20** binds to EDO **19**, suggesting that the lack of EDO-promoted reactivity of **3** is due to the steric profile of the neosilyl ligand. These results highlight the potential utility of light-promoted processes to achieve $C(sp^3)-C(sp^3)$ bond formation within sterically demanding environments.

We then compared the efficiency of light-promoted bond formation to that of EDO-induced reductive elimination in

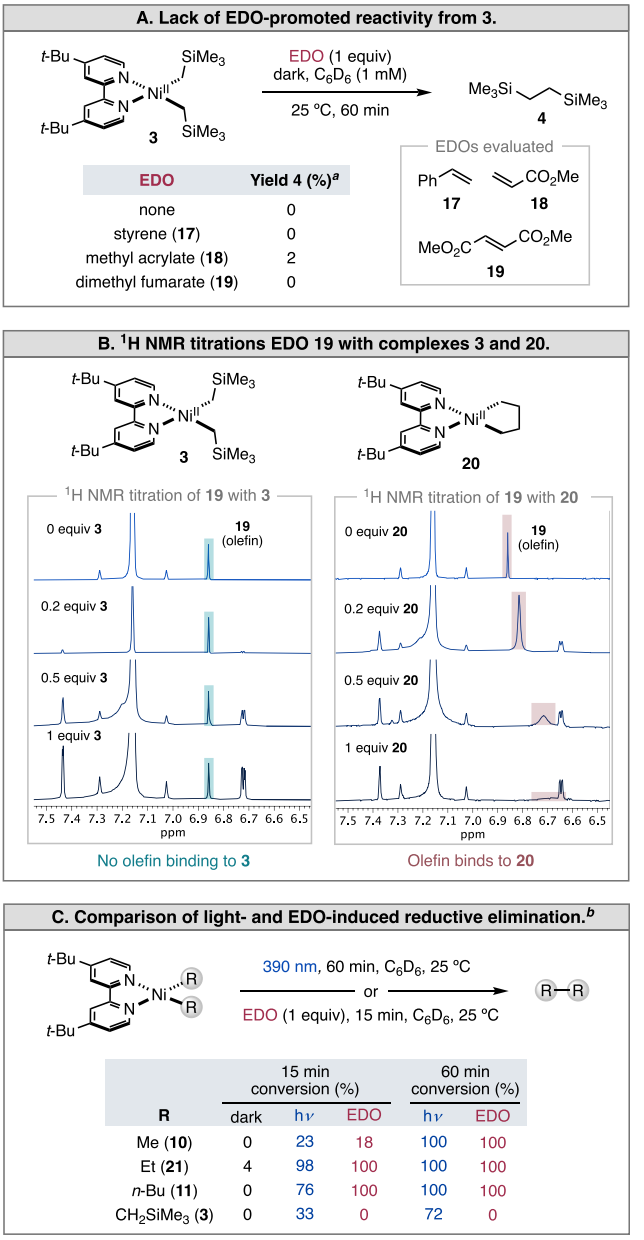

Figure 8. (A) Treatment of **3** with a variety of π-accepting electron-deficient olefins (EDOs). (a) ^1H NMR yield based on the toluene internal standard. (B) Comparative ^1H NMR titration study (in C_6D_6) of **19** with **3** and **20** highlighting binding to **20** but not **3**. (C) Comparison of the activation of various dialkyl Ni^{II} complexes with EDOs and light. (b) Percent conversion at 15 and 60 min determined by ^1H NMR with toluene as an internal standard.

scenarios where both strategies are applicable. To this end, we prepared a library of dialkyl Ni^{II} complexes featuring alkyl groups of varying steric encumbrance. After 15 min, both $(^{t\text{-}Bu}bpy)Ni^{II}(Me)_2$ (**10**) and $(^{t\text{-}Bu}bpy)Ni^{II}(Et)_2$ (**21**) afford similar conversion at 15 and 60 min, whether treated with 390 nm light or 1 equiv of dimethylfumarate (**19**) (Figure 8C). However, photolysis experiments carried out without gaseous headspace highlight that the irradiation of **21** also leads to the formation of ethylene (Supporting Information, Section 5). Interestingly, as was also observed by Yamamoto and co-workers, **10** is less reactive than **18**. For $(^{t\text{-}Bu}bpy)Ni^{II}(n\text{-}Bu)_2$ (**11**), *n*-octane was formed nearly quantitatively in 15 min with the addition of **19**, whereas photolysis affords 76% and 100%

https://doi.org/10.1021/jacs.5c09925
J. Am. Chem. Soc. XXXX, XXX, XXX−XXX

conversion after 15 and 60 min, respectively. As stated above, ($^{t\text{-Bu}}$bpy)Ni^{II}(CH_2SiMe_3)$_2$ is unreactive with **19**, but bond formation is still achieved upon irradiation. In summary, while both photochemical- and EDO-induced reductive elimination are C(sp^3)−C(sp^3) bond formation strategies applicable when coupling sterically unencumbered alkyl fragments, the photochemical approach is advantageous in sterically challenging systems wherein EDO binding is unfavorable.

CONCLUSIONS

In summary, we report a thorough investigation into a photochemical reductive elimination from bpy-ligated Ni^{II} dialkyl complexes, overcoming the typically insurmountable thermal barriers for such transformations. Through a detailed mechanistic investigation, we identified a photolysis/radical rebound mechanism to be operative. This mechanism is supported by a wavelength-dependent reactivity cutoff, quantitative formation of a Ni^0 photoproduct, and product distributions in crossover studies. This direct means of forming challenging C−C bonds offers a complementary reactivity paradigm to established ligand-focused strategies. In particular, the photochemical approach can circumvent steric hindrances that limit EDO binding, providing an alternative to bond formation from sterically crowded metal centers. By leveraging photochemistry, we hope to open new opportunities to expand the scope of Ni-catalyzed cross-couplings in systems where challenging C(sp^3)−C(sp^3) bond formation is otherwise inaccessible

ASSOCIATED CONTENT

Supporting Information

The Supporting Information is available free of charge at https://pubs.acs.org/doi/10.1021/jacs.5c09925.

Experimental procedures, experimental and computational data, and characterization and spectral data for new compounds (PDF)

Data from quantum mechanics calculations (XLSX)

Coordinates of computed structures (ZIP)

AUTHOR INFORMATION

Corresponding Authors

Ryan G. Hadt − *Division of Chemistry and Chemical Engineering, Arthur Amos Noyes Laboratory of Chemical Physics, California Institute of Technology, Pasadena, California 91125, United States;* orcid.org/0000-0001-6026-1358; Email: rghadt@caltech.edu

Abigail G. Doyle − *Department of Chemistry and Biochemistry, University of California Los Angeles, Los Angeles, California 90095, United States;* orcid.org/0000-0002-6641-0833; Email: abigaildoyle@g.ucla.edu

Authors

Alexander Q. Cusumano − *Department of Chemistry and Biochemistry, University of California Los Angeles, Los Angeles, California 90095, United States*

Braden C. Chaffin − *Department of Chemistry and Biochemistry, University of California Los Angeles, Los Angeles, California 90095, United States*

David A. Cagan − *Division of Chemistry and Chemical Engineering, Arthur Amos Noyes Laboratory of Chemical Physics, California Institute of Technology, Pasadena, California 91125, United States;* orcid.org/0000-0002-4719-2789

Stephen DiLuzio − *Division of Chemistry and Chemical Engineering, Arthur Amos Noyes Laboratory of Chemical Physics, California Institute of Technology, Pasadena, California 91125, United States*

Erica Sutcliffe − *Division of Chemistry and Chemical Engineering, Arthur Amos Noyes Laboratory of Chemical Physics, California Institute of Technology, Pasadena, California 91125, United States*

Complete contact information is available at: https://pubs.acs.org/10.1021/jacs.5c09925

Author Contributions

‡A.Q.C. and B.C.C. contributed equally.

Author Contributions

⊥D.A.C., S.D., and E.S. contributed equally.

Notes

The authors declare no competing financial interest.

ACKNOWLEDGMENTS

We thank T. Judah Raab for helpful discussions. We thank Kessil (DiCon Fiberoptics, Inc.) for support with custom wavelength LEDs for wavelength dependence studies. The mechanistic studies were supported as a part of BioLEC, an Energy Frontier Research Center funded by the U.S. Department of Energy, Office of Science, under grant no.: DE-SC0019370 to A.G.D. A.G.D. also acknowledges NIGMS R35 GM126986 for the organometallic synthesis and reactivity studies. A.Q.C. acknowledges financial support from the National Institute of Health under the Ruth L. Kirschstein National Research Service Award (NRSA) fellowship (F32GM151836). B.C.C. acknowledges financial support from NSF Grant DGE-2034835. These studies were supported by shared instrumentation grants from the National Science Foundation under equipment grants CHE-1048804 and 2117480, along with the NIH Office of Research Infrastructure Program supergrant S10OD028644. R.G.H. acknowledges support from NIGMS R35-GM142595 for photochemical and transient spectroscopic studies.

REFERENCES

(1) (a) Chan, A. Y.; Perry, I. B.; Bissonnette, N. B.; Buksh, B. F.; Edwards, G. A.; Frye, L. I.; Garry, O. L.; Lavagnino, M. N.; Li, B. X.; Liang, Y.; Mao, E.; Millet, A.; Oakley, J. V.; Reed, N. L.; Sakai, H. A.; Seath, C. P.; MacMillan, D. W. C. Metallaphotoredox: The Merger of Photoredox and Transition Metal Catalysis. *Chem. Rev.* **2022**, *122*, 1485−1542. (b) Cavalcanti, L. N.; Molander, G. A. Photoredox Catalysis in Nickel-Catalyzed Cross-Coupling. *Top. Curr. Chem.* **2016**, *374*, 39.

(2) (a) Tasker, S. Z.; Standley, E. A.; Jamison, T. F. Recent Advances in Homogeneous Nickel Catalysis. *Nature* **2014**, *509*, 299−309. (b) Diccianni, J.; Lin, Q.; Diao, T. Mechanisms of Nickel-Catalyzed Coupling Reactions and Applications in Alkene Functionalization. *Acc. Chem. Res.* **2020**, *53*, 906−919. (c) Diccianni, J. B.; Diao, T. Mechanisms of Nickel-Catalyzed Cross-Coupling Reactions. *Trends in Chemistry* **2019**, *1*, 830−844. (d) Lin; Liu, L.; Fu, Y.; Luo, S.-W.; Chen, Q.; Guo, Q.-X. Comparing Nickel- and Palladium-Catalyzed Heck Reactions. *Organometallics* **2004**, *23*, 2114−2123.

(3) Sun, R.; Qin, Y.; Nocera, D. G. General Paradigm in Photoredox Nickel-Catalyzed Cross-Coupling Allows for Light-Free Access to Reactivity. *Angew. Chem., Int. Ed.* **2020**, *59*, 9527−9533.

(4) Wenger, O. S. Photoactive Nickel Complexes in Cross-Coupling Catalysis. *Chem. - Eur. J.* **2021**, *27*, 2270−2278.

(5) (a) Ting, S. I.; Garakyaraghi, S.; Taliaferro, C. M.; Shields, B. J.; Scholes, G. D.; Castellano, F. N.; Doyle, A. G. ^{3}d-d Excited States of Ni(II) Complexes Relevant to Photoredox Catalysis: Spectroscopic Identification and Mechanistic Implications. *J. Am. Chem. Soc.* **2020**, *142*, 5800−5810. (b) Cagan, D. A.; Bím, D.; Silva, B.; Kazmierczak, N. P.; McNicholas, B. J.; Hadt, R. G. Elucidating the Mechanism of Excited-State Bond Homolysis in Nickel−Bipyridine Photoredox Catalysts. *J. Am. Chem. Soc.* **2022**, *144*, 6516−6531. (c) Bím, D.; Luedecke, K. M.; Cagan, D. A.; Hadt, R. G. Light Activation and Photophysics of a Structurally Constrained Nickel(II)−Bipyridine Aryl Halide Complex. *Inorg. Chem.* **2024**, *63*, 4120−4131. (d) Cagan, D. A.; Stroscio, G. D.; Cusumano, A. Q.; Hadt, R. G. Multireference Description of Nickel−Aryl Homolytic Bond Dissociation Processes in Photoredox Catalysis. *J. Phys. Chem. A* **2020**, *124*, 9915−9922. (e) Cagan, D. A.; Bím, D.; McNicholas, B. J.; Kazmierczak, N. P.; Oyala, P. H.; Hadt, R. G. Photogenerated Ni(I)−Bipyridine Halide Complexes: Structure−Function Relationships for Competitive C-(sp^2)−Cl Oxidative Addition and Dimerization Reactivity Pathways. *Inorg. Chem.* **2023**, *62*, 9538−9551. Recently, this paradigm has also been demonstrated with [2.2]pyridinophane-ligated Ni^{II} aryl halide complexes: (f) Westawker, L. P.; Bouley, B. S.; Vura-Weis, J.; Mirica, L. M. Photochemistry of Ni(II) Tolyl Chlorides Supported by Bidentate Ligand Frameworks. *J. Am. Chem. Soc.* **2025**, *147*, 17315−17329.

(6) (a) Song, G.; Li, Q.; Nong, D.-Z.; Song, J.; Li, G.; Wang, C.; Xiao, J.; Xue, D. Ni-Catalyzed Photochemical C−N Coupling of Amides with (Hetero)Aryl Chlorides. *Chem. - Eur. J.* **2023**, *29*, No. e202300458. The Pieber lab has demonstrated the analogous Ni−X homolysis at longer wavelengths (440 nm) by employing carbazole substituted bipyridine ligands: (b) Cavedon, C.; Gisbertz, S.; Reischauer, S.; Vogl, S.; Sperlich, E.; Burke, J. H.; Wallick, R. F.; Schrottke, S.; Hsu, W.-H.; Anghileri, L.; Pfeifer, Y.; Richter, N.; Teutloff, C.; Müller-Werkmeister, H.; Cambié, D.; Seeberger, P. H.; Vura-Weis, J.; van der Veen, R. M.; Thomas, A.; Pieber, B. Intraligand Charge Transfer Enables Visible-Light-Mediated Nickel-Catalyzed Cross-Coupling Reactions. *Angew. Chem., Int. Ed.* **2022**, *61*, No. e202211433. For examples with bathocuproine-ligated Ni^{II} (c) Powers, D. C.; Anderson, B. L.; Nocera, D. G. Two-Electron HCl to H_2 Photocycle Promoted by Ni(II) Polypyridyl Halide Complexes. *J. Am. Chem. Soc.* **2013**, *135* (50), 18876−18883.

(7) (a) Anghileri, L.; Baunis, H.; Bena, A. R.; Giannoudis, C.; Burke, J. H.; Reischauer, S.; Merschjann, C.; Wallick, R. F.; Al Said, T.; Adams, C. E.; Simionato, G.; Kovalenko, S.; Dell'Amico, L.; van der Veen, R. M.; Pieber, B. Evidence for a Unifying NiI/NiIII Mechanism in Light-Mediated Cross-Coupling Catalysis. *J. Am. Chem. Soc.* **2025**, *147*, 13169−13179. (b) Yang, L.; Lu, H.-H.; Lai, C.-H.; Li, G.; Zhang, W.; Cao, R.; Liu, F.; Wang, C.; Xiao, J.; Xue, D. Light-Promoted Nickel Catalysis: Etherification of Aryl Electrophiles with Alcohols Catalyzed by a NiII-Aryl Complex. *Angew. Chem., Int. Ed.* **2020**, *59*, 12714−12719.

(8) (a) Cusumano, A. Q.; Chaffin, B. C.; Doyle, A. G. Mechanism of Ni-Catalyzed Photochemical Halogen Atom-Mediated C(sp^3)−H Arylation. *J. Am. Chem. Soc.* **2024**, *146*, 15331−15344. (b) McManus, B. D.; Hung, L. C.; Taylor, O. R.; Nguyen, P. Q.; Cedeño, A. L.; Arriola, K.; Bradley, R. D.; Saucedo, P. J.; Hannan, R. J.; Luna, Y. A.; Farias, P.; Bahamonde, A. Mechanistic Interrogation of Photochemical Nickel-Catalyzed Tetrahydrofuran Arylation Leveraging Enantioinduction Data. *J. Am. Chem. Soc.* **2024**, *146*, 32135−32146.

(9) Shin, J.; Lee, J.; Suh, J.-M.; Park, K. Ligand-Field Transition-Induced C−S Bond Formation from Nickelacycles. *Chem. Sci.* **2021**, *12*, 15908−15915.

(10) (a) Welin, E. R.; Le, C.; Arias-Rotondo, D. M.; McCusker, J. K.; MacMillan, D. W. C. Photosensitized, Energy Transfer-Mediated Organometallic Catalysis through Electronically Excited Nickel(II). *Science* **2017**, *355*, 380−385. (b) Tian, L.; Till, N. A.; Kudisch, B.; MacMillan, D. W. C.; Scholes, G. D. Transient Absorption Spectroscopy Offers Mechanistic Insights for an Iridium/Nickel-Catalyzed C−O Coupling. *J. Am. Chem. Soc.* **2020**, *142*, 4555−4559.

(11) (a) Ma, P.; Wang, S.; Chen, H. Reactivity of Transition-Metal Complexes in Excited States: C−O Bond Coupling Reductive Elimination of a Ni(II) Complex is Elicited by the Metal-to-Ligand Charge Transfer State. *ACS Catal.* **2020**, *10*, 1−6. (b) Dong, Y.-J.; Zhao, Z.-W.; Geng, Y.; Su, Z.-M.; Zhu, B.; Guan, W. Theoretical Insight on the High Reactivity of Reductive Elimination of Ni^{III} Based on Energy- and Electron-Transfer Mechanisms. *Inorg. Chem.* **2023**, *62*, 1156−1164.

(12) Kancherla, R.; Muralirajan, K.; Maity, B.; Karuthedath, S.; Kumar, G. S.; Laquai, F.; Cavallo, L.; Rueping, M. Mechanistic Insights into Photochemical Nickel-Catalyzed Cross-Couplings Enabled by Energy Transfer. *Nat. Commun.* **2022**, *13*, 2737.

(13) (a) Low, J. J.; Goddard, W. A. Theoretical Studies of Oxidative Addition and Reductive Elimination. 2. Reductive Coupling of Hydrogen-Hydrogen, Hydrogen-Carbon, and Carbon-Carbon Bonds from Palladium and Platinum Complexes. *Organometallics* **1986**, *5*, 609−622. (b) Low, J. J.; Goddard, W. A. Theoretical Studies of Oxidative Addition and Reductive Elimination. 3. Carbon-Hydrogen and Carbon-Carbon Reductive Coupling from Palladium and Platinum Bis(Phosphine). *Complexes. J. Am. Chem. Soc.* **1986**, *108*, 6115−6128.

(14) (a) Yamamoto, T.; Yamamoto, A.; Ikeda, S. Organo (Dipyridyl) Nickel Complexes. I. Stability and Activation of the Alkyl-Nickel Bonds of Dialkyl (Dipyridyl) Nickel by Coordination with Various Substituted Olefins. *J. Am. Chem. Soc.* **1971**, *93*, 3350−3359. (b) Yamamoto, T.; Abla, M. Reductive Elimination of Et—Et from $NiEt_2$(Bpy) Promoted by Electron-Accepting Aromatic Compounds. *J. Organomet. Chem.* **1997**, *535*, 209−211.

(15) Ju, L.; Hu, C. T.; Diao, T. Strategies for Promoting Reductive Elimination of Bi- and Bis-Oxazoline Ligated Organonickel Complexes. *Organometallics* **2022**, *41*, 1748−1753.

(16) Dawson, G. A.; Seith, M. C.; Neary, M. C.; Diao, T. Redox Activity and Potentials of Bidentate N-Ligands Commonly Applied in Nickel-Catalyzed Cross-Coupling Reactions. *Angew. Chem., Int. Ed.* **2024**, *63*, No. e202411110.

(17) Sun, J.; He, J.; Massaro, L.; Cagan, D. A.; Tsien, J.; Wang, Y.; Attard, F. C.; Smith, J. E.; Lee, J. S.; Kawamata, Y.; Baran, P. S. Stereoretentive Radical Cross-Coupling. *Nature* **2025**, *642*, 85−91.

(18) Yerbulekova, A.; Moshood, Y.; Griego, L.; Shafaat, H. S.; Mirica, L. M. Spectroscopic and Computational Interrogation of a High-Valent Nickel-Dialkyl Complex Indicates Electronic Structure Asymmetry Drives C−C Bond Formation Reactivity. *J. Am. Chem. Soc.* **2025**, *147*, 7317−7324.

(19) Computed at the TPSSh-D4/def2-TZVPP/CPCM(benzene)//PBE-D4/def2-TZVP(Ni), def2-SV(P)/CPCM(benzene) level of theory. See supporting information section 7 for further details.

(20) Addition of COD or benzophenone as π-accepting ligand to the photoproduct also produces a UV−vis spectrum in accord with prior reports of bipyridine Ni^0(L) complexes. King, A. E.; Stieber, S. C. E.; Henson, N. J.; Kozimor, S. A.; Scott, B. L.; Smythe, N. C.; Sutton, A. D.; Gordon, J. C. Ni(Bpy)(Cod): A Convenient Entryway into the Efficient Hydroboration of Ketones, Aldehydes, and Imines. *Eur. J. Inorg. Chem.* **2016**, *2016*, 1635−1640.

(21) Ni^{II}−CH_3 photolysis also later reported by Oderinde and co-workers: Oderinde, M. S.; Jin, S.; Das, J.; Jorge, C.; Yip, S.; Ramirez, A.; Wu, D.-R.; Li, Y.; Kempson, J.; Meanwell, N. A.; Mathur, A.; Dhar, T. G. M. Photo-Initiated Nickel Catalysis (PiNiC): Unmasking Dimethylnickel with Light. *ACS Catal.* **2022**, *12*, 12511−12520.

(22) (a) Huang, X.; Groves, J. T. Beyond Ferryl-Mediated Hydroxylation: 40 Years of the Rebound Mechanism and C−H Activation. *J. Biol. Inorg. Chem.* **2017**, *22*, 185−207. (b) Joy, J.; Schaefer, A. J.; Teynor, M. S.; Ess, D. H. Dynamical Origin of Rebound versus Dissociation Selectivity during Fe-Oxo-Mediated C−H Functionalization Reactions. *J. Am. Chem. Soc.* **2024**, *146*, 2452−2464.

(23) The lower yield of **14** compared to **12** may be affected by a slower rate of cage escape for the larger *n*-Bu$^\bullet$ radical. (a) Herk, L.; Feld, M.; Szwarc, M. Studies of "Cage" Reactions. *J. Am. Chem. Soc.*

https://doi.org/10.1021/jacs.5c09925
J. Am. Chem. Soc. XXXX, XXX, XXX−XXX

1961, *83* (14), 2998−3005. (b) Braden, D. A.; Parrack, E. E.; Tyler, D. R. Solvent Cage Effects. I. Effect of Radical Mass and Size on Radical Cage Pair Recombination Efficiency. II. Is Geminate Recombination of Polar Radicals Sensitive to Solvent Polarity? *Coord. Chem. Rev.* **2001**, *211*, 279−294.

(24) (a) Lin, Q.; Spielvogel, E. H.; Diao, T. Carbon-Centered Radical Capture at Nickel(II) Complexes: Spectroscopic Evidence, Rates, and Selectivity. *Chem.* **2023**, *9*, 1295−1308. (b) Al Zubaydi, S.; Waske, S.; Akyildiz, V.; Starbuck, H. F.; Majumder, M.; Moore, C. E.; Kalyani, D.; Sevov, C. S. Reductive Alkyl−Alkyl Coupling from Isolable Nickel−Alkyl Complexes. *Nature* **2024**, *634*, 585−591.

(25) Shields, B. J.; Kudisch, B.; Scholes, G. D.; Doyle, A. G. Long-Lived Charge-Transfer States of Nickel(II) Aryl Halide Complexes Facilitate Bimolecular Photoinduced Electron Transfer. *J. Am. Chem. Soc.* **2018**, *140*, 3035−3039.

(26) Day, C. S.; Ton, S. J.; McGuire, R. T.; Foroutan-Nejad, C.; Martin, R. Reductive Elimination from Sterically Encumbered Ni−Polypyridine Complexes. *Organometallics* **2022**, *41*, 2662−2667.

(27) (a) Yamamoto, T.; Yamamoto, A.; Ikeda, S. Organo (Dipyridyl) Nickel Complexes. II. Stabilities of Olefin-Nickel Bonds in Olefin-Coordinated Dipyridylnickel and Dialkyl (Dipyridyl) Nickel Complexes. *J. Am. Chem. Soc.* **1971**, *93*, 3360−3364. (b) Estrada, J. G.; Williams, W. L.; Ting, S. I.; Doyle, A. G. Role of Electron-Deficient Olefin Ligands in a Ni-Catalyzed Aziridine Cross-Coupling to Generate Quaternary Carbons. *J. Am. Chem. Soc.* **2020**, *142*, 8928−8937. Note that electron-deficient olefins may also induce reductive elimination due to generation of a higher-valent intermediate: (c) Tatsumi, K.; Nakamura, A.; Komiya, S.; Yamamoto, A.; Yamamoto, T. An Associative Mechanism for Reductive Elimination of d^8 $NiR_2(PR_3)_2$. *J. Am. Chem. Soc.* **1984**, *106*, 8181−8188. (d) Tatsumi, K.; Hoffmann, R.; Yamamoto, A.; Stille, J. K. Reductive Elimination of d^8-Organotransition Metal Complexes. *Bull. Chem. Soc. Jpn.* **1981**, *54*, 1857−1867. (e) Komiya, S.; Abe, Y.; Yamamoto, A.; Yamamoto, T. Phosphine-Induced Reductive Elimination from Cis-Arylmethylnickel(II) Complexes Having a 1,2-Bis-(Dimethylphosphino)Ethane Ligand. *Organometallics* **1983**, *2*, 1466−1468.

(28) Giovannini, R.; Stüdemann, T.; Devasagayaraj, A.; Dussin, G.; Knochel, P. New Efficient Nickel-Catalyzed Cross-Coupling Reaction between Two $C(sp^3)$ Centers. *J. Org. Chem.* **1999**, *64*, 3544−3553.

https://doi.org/10.1021/jacs.5c09925
J. Am. Chem. Soc. XXXX, XXX, XXX−XXX